Efficiency Estimations for a Broadband 7 THz Radiation Source with GaAs/AlGaAs Parabolic Quantum Wells

Reeno Reeder[1], Zoran Ikonić[2], Paul Harrison[2], Andres Udal[1], and Enn Vemre[1]

1 - The Electronics Department, Tallinn University of Technology,
Ehitajate tee 5, Tallinn 19086, Estonia

1918
TALLINNA TEHNIKAÜLIKOOL
TALLINN UNIVERSITY OF TECHNOLOGY

Department of Electronics

2 - The Institute of Microwaves and Photonics, School of Electronic and Electrical Engineering, University of Leeds, Leeds LS2 9JT, UK

School of Electronic and Electrical Engineering

INTRODUCTION – Questions and Goals

! STARTING POINTS

- Parabolic QW with equispaced energy eigenvalues – suitable for a radiation source with a rather well controlled spectrum
- Population inversion not needed, working temperature not as critical as in lasers
- Electrons may be excited into higher states (subbands) by lateral current
- The digitally graded potential distribution, e.g. on GaAs/AlGaAs system, may give quasi-parabolic QW with a reasonably low deviation (<5%) of the energy steps:

  • R.Reeder, A.Udal, E.Velmre, P.Harrison. Proc. of 10th Baltic Electronics Conf. BEC2006, Tallinn, Estonia, 2-4. Oct. 2006, pp. 51-54 (on-line available through IEEE Xplore)

? QUESTIONS

- What could be the radiation output of a broadband incoherent 7 Thz source based on GaAs/Al0.42Ga0.58As digitally graded parabolic QW layer pumped by the lateral current?
- Can this device be effective at room temperature and above?

! GOAL

- Develop a medium-complex approach to estimate radiation efficiency

----

FULL PAPER TO BE PUBLISHED:

• R.Reeder, Z.Ikonić, P.Harrison, A.Udal, E.Velmre. Laterally pumped GaAs/AlGaAs quantum wells as sources of broadband THz radiation, accepted for publication in Journal of Applied Physics.

INTRODUCTION – The Device

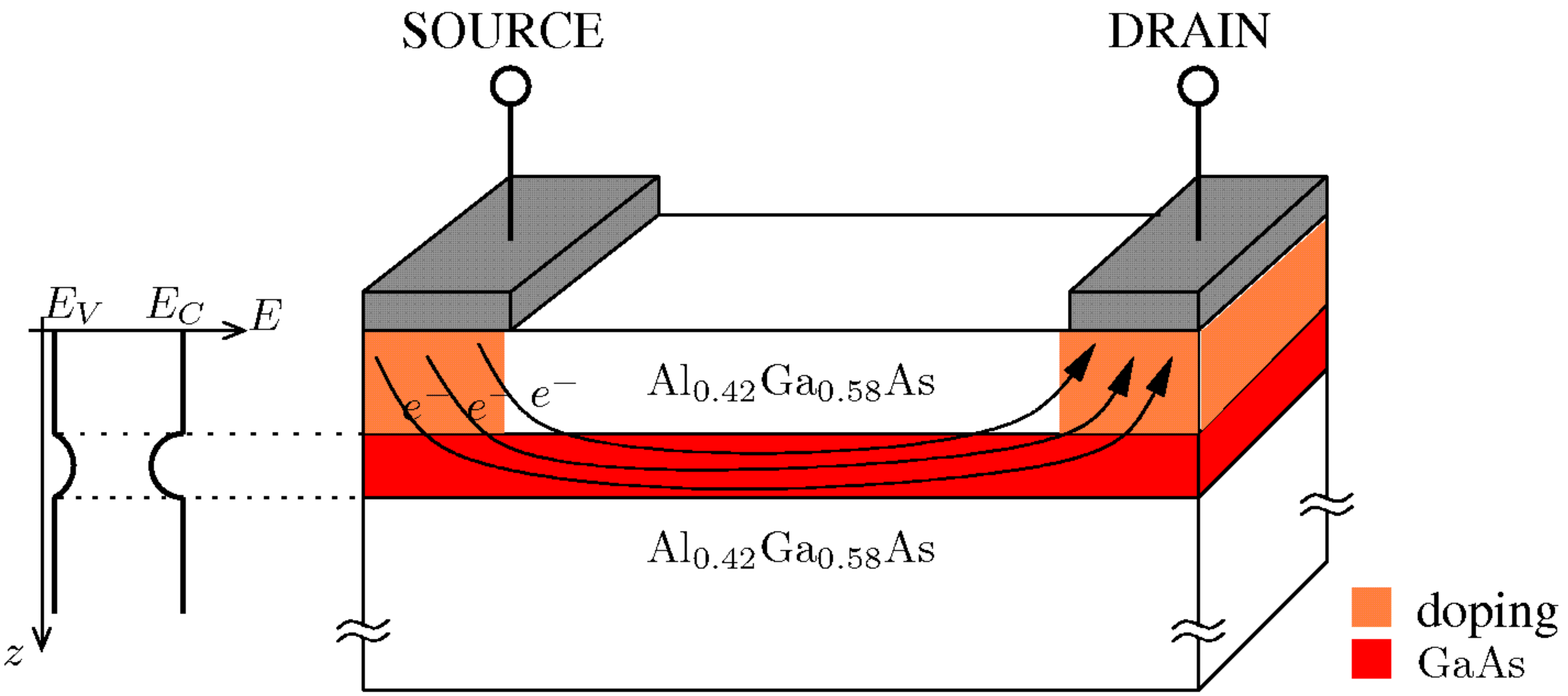

FIG. The possible construction of the laterally pumped quantum well emitter. The doping (e.g. 10^{12} cm^{-2}) should be localised in 2D quantum layer and in the regions under the contacts. The quantum well layer, marked by red, actually contains a fine structure of potential barriers and wells created by GaAs/$Al_{0.42}Ga_{0.58}As$ composition changes in z-direction. Approximate width of the QW layer is 60 nm.

PRE-WORK – Constructing the Digitally Graded Quasi-Parabolic QW

Results from: • **R.Reeder, A.Udal, E.Velmre, P.Harrison. Proc. of 10th Baltic Electronics Conf. BEC2006, Tallinn, Estonia, 2-4. Oct. 2006, pp. 51-54 (on-line available through IEEE Xplore)**

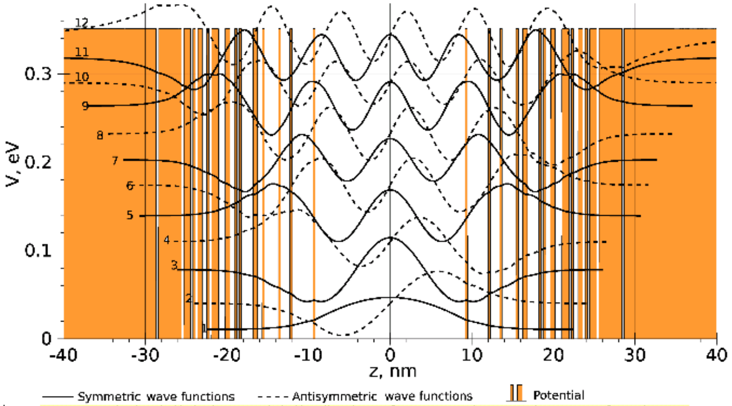

Fig. Optimised digital potential distribution of type 1 and respective wave functions (in arbitrary units), rised by energy eigenvalues. 7 THz quasi-parabolic quantum well.

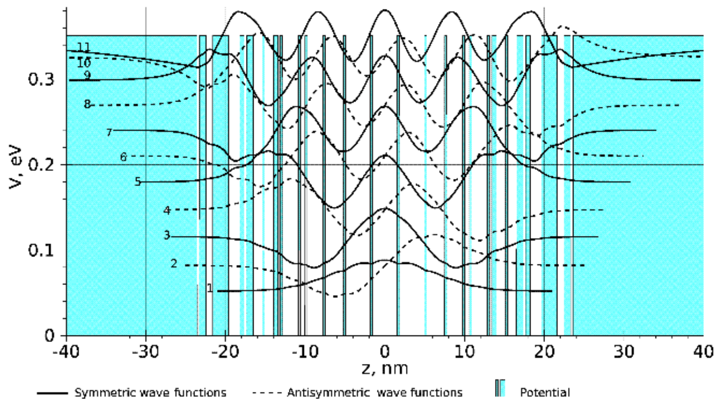

Fig. Optimised digital potential distribution of type 2 and respective wave functions (in arbitrary units), rised by energy eigenvalues. 7 THz quasi-parabolic quantum well.

CONCLUDING RESULTS 1
Obtained "best" spacings of energy levels

$$\Delta E_i \equiv E_{i+1} - E_i = f(E)$$

Fig. Obtained most uniform energy levels spacings ΔE for digitised distributions of type 1 and 2.

Yellow bands: ±5%

Horisontal axis is energy itself what varies from zero (QW bottom) to 0.3509 eV (QW top)

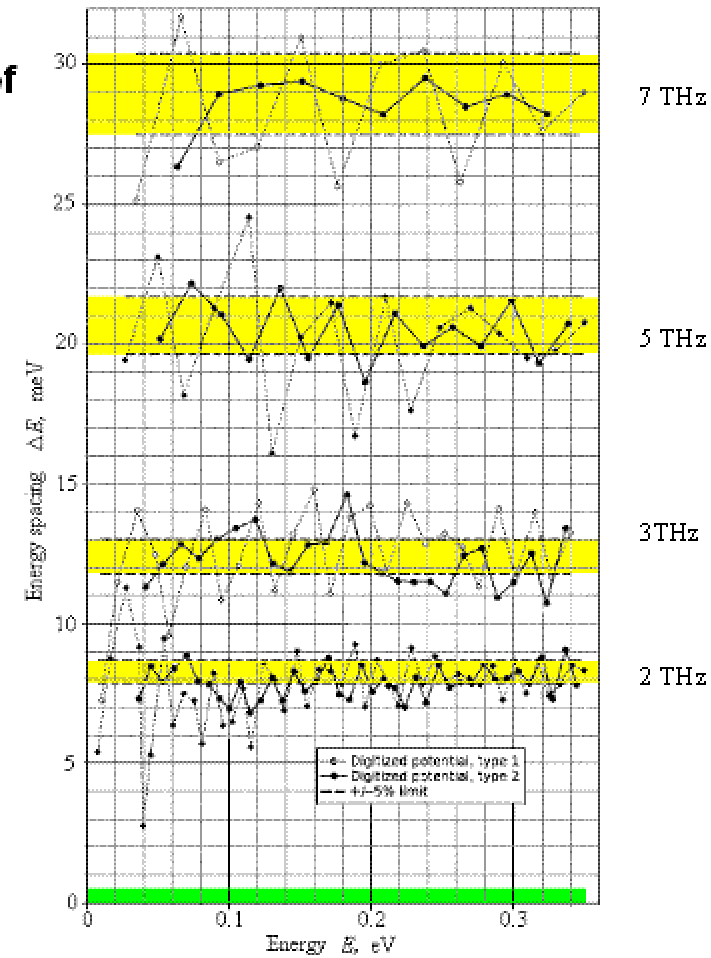

FIGS. The wavefunctions and the best (uniformly distributed) energy eigenvalues obtained for digitally graded QW. Below in this study we use type 2 distribution for 7 THz where we add into consideration also the bound state no. 12 which energy is very close to QW top 0.3509 eV.

MODEL – The Transitions between the Subbands

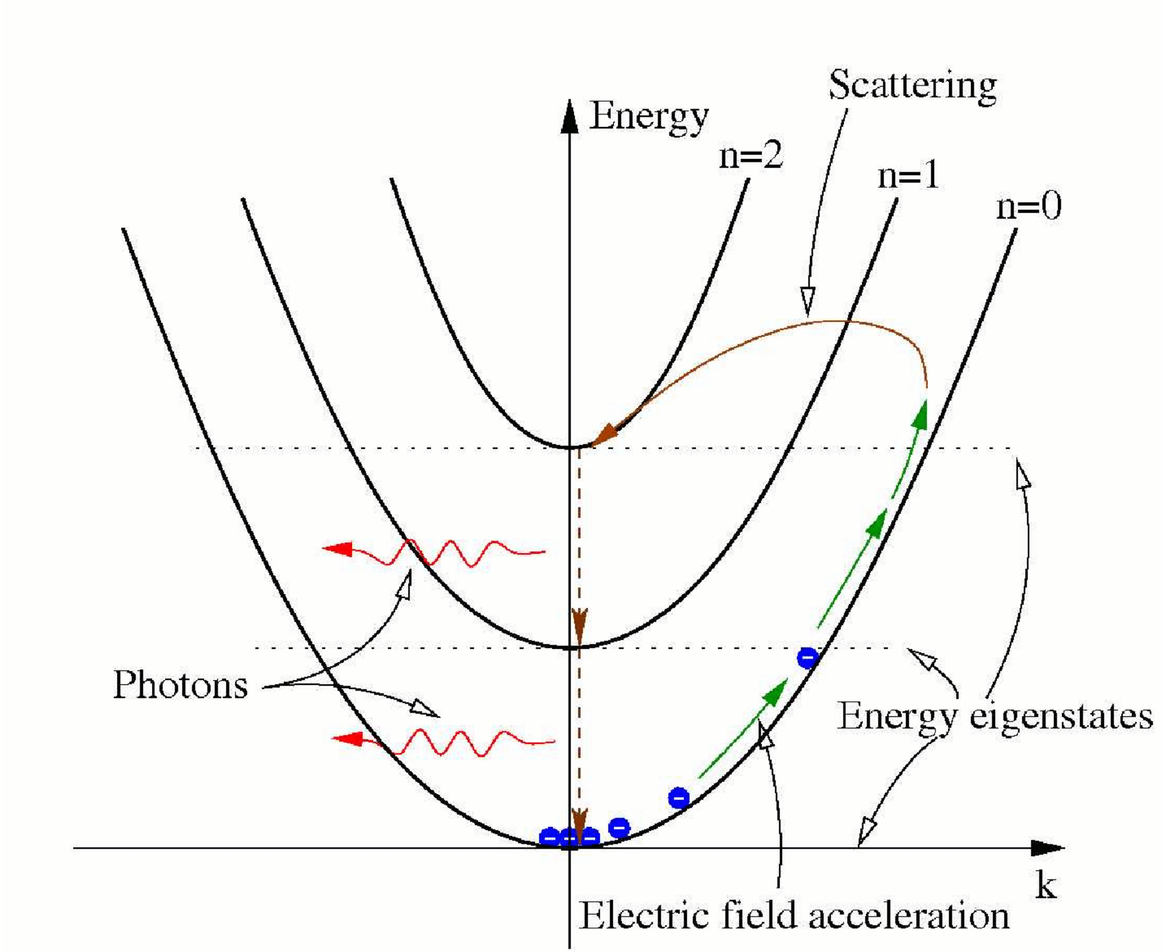

FIG. Illustration of considered subband excitation and relaxation processes. Here *k* denotes electron wavenumber in-plane directions *x* and/or *y*. Longitudinal polar optic phonon and deformation potential acoustic phonon intersubband scattering mechanisms are taken into account (for both the phonon emission and absorption cases)*. By using the shifted Fermi-Dirac distributions for every subband the averaged scattering rates for all intersubband transitions **i** → **f** were found and used as coefficients in rate equation system. In present calculations no. of bound states (subbands) was 12 and no. of quasi-continuum states (subbands) was also taken 12.

- **- P. Harrison. Quantum Wells, Wires and Dots, 2005, sections 9.4 and 9.9.**

MODEL – The Constructed Empirical $v_d(F)$ and $T_e(F)$

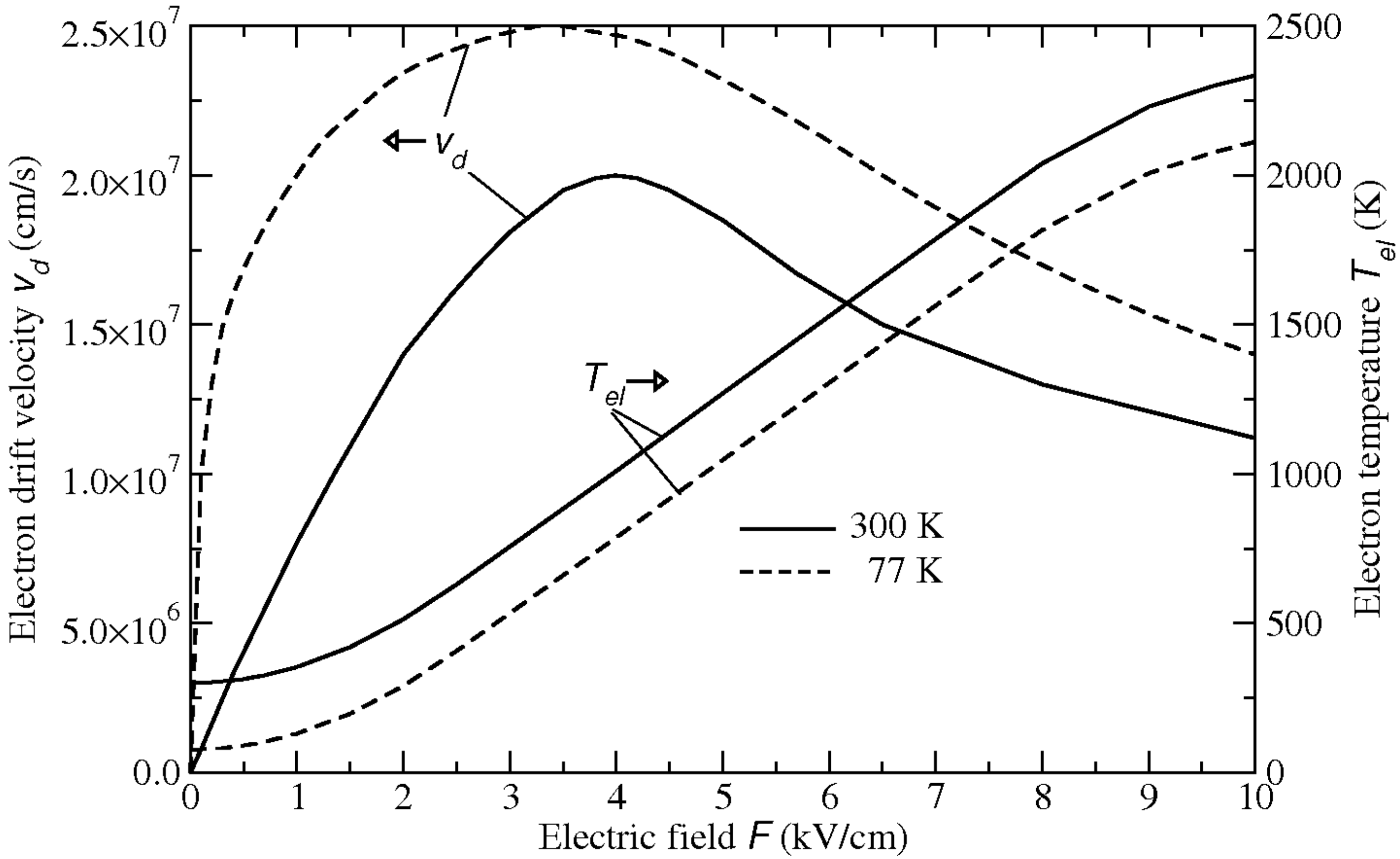

FIG. The constructed electron drift velocity and electron temperature dependencies on lateral electric field strength value. These approximate curves take into account theoretical and experimental data from several studies of different authors. These 2 parameters (the same for all subbands) were used for shifted Fermi-Dirac distributions to find averaged intersubband scattering rates. Using of this two empirical parameters allowed us in the present preliminary calculations to keep complexity of models and amount of necessary computer time in reasonable limits.

MODEL – The General Lines

- Specify potential in z-direction to obtain wanted spacing of energy eigenvalues (e.g. ΔE = 28.95 meV for 7 THz). In the case of 42% Al the QW depth is 0.3509 eV which yields 12 bound states (subbands). Add some number (e.g. 12) quasi-continuum states in a wider infinite box (e.g. 200 nm).
- Assume fixed total electron concentration (e.g. $nsum = 10^{12}$ cm^{-2}) for all subbands. This is technologically defined by the doping in QW layer.
- Construct the RATE EQUATIONS SYSTEM with using AVERAGED INTERSUBBAND SCATTERING RATES as the coefficients to describe electron transition flows between all subbands $i \rightarrow f$. Solution is the electron concentrations ni (populations) in each subband.
- For the "raw" scattering rates (which depend on in-plane wavenumber ki of electron in initial i-subband) use longitudinal polar optic phonon and deformation potential acoustic phonon intersubband scattering mechanisms (for both the phonon emission and absorption cases).
- To find averaged scattering rates over all ki values in every subband assume the applicability of the SHIFTED FERMI-DIRAC DISTRIBUTIONS. This distribution takes into account the "k-shift $kx0$" along x-direction representing the drift of electrons caused by the lateral electric field and as well the rise of electron temperature Te over the lattice temperature due to the lateral field.
- Assume that shifted Fermi-Dirac distribution PARAMETERS $kx0$ AND Te ARE THE SAME FOR ALL SUBBANDS. Allow some changes in individual Fermi energies EFi for every subband to avoid conflict with populations obtained from rate equations.
- Simplifying assumption: use EMPIRICAL DRIFT VELOCITY VS FIELD $vd(F)$ and EMPIRICAL ELECTRON TEMPERATURE VS FIELD $Te(F)$ from the studies of other authors.
- OPTICAL OUTPUT calculate on the basis of spontaneous photon emission rates for all downward $i > f$ transitions. Assume Lorentzian-type spectrum with broadening parameter Γ= 5meV.

MODEL – The Important Formulae

The rate equations:

$$\frac{\mathrm{d}n_f}{\mathrm{d}t} = \sum_{i=1}^{N} \frac{1}{\tau_{if}} n_i - n_f \sum_{i=1}^{N} \frac{1}{\tau_{fi}} = 0$$

The shifted Fermi-Dirac distribution:

$$f^{sFD}(\mathbf{k}) = \left[1 + \exp \frac{E_{n0} + \frac{\hbar^2\left((k_x - k_0(F, T_{latt}))^2 + k_y^2\right)}{2m*} - E_{F_n}}{k_B T_{el}(F, T_{latt})} \right]^{-1}$$

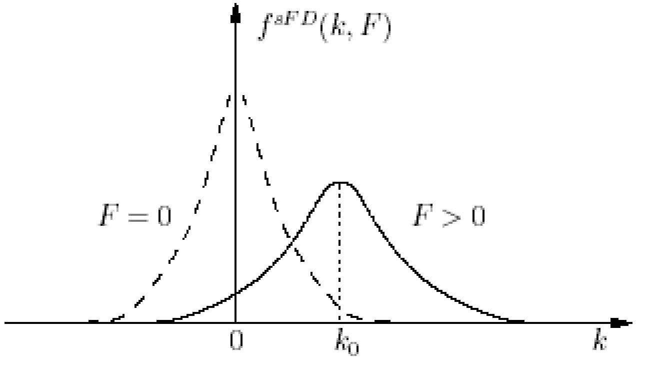

with $v_d = \hbar k_0 / m^*$ $\quad k_0\left(F, T_{latt}\right)$ and $T_{el}\left(F, T_{latt}\right)$

The concentration (population) from the F-D:

$$n_i = \frac{2}{4\pi^2} \int_{k_x, k_y} f^{sFD}(\mathbf{k}) dk_x dk_y$$

The optical output power:

$$P_{\text{total}} = \sum_{i>f}^{N} \frac{n_i}{\tau_{if}^{\text{rad}}} \hbar\omega_{if}$$

with spontaneous transition lifetime

$$\frac{1}{\tau_{if}^{\text{rad}}} = \frac{e^2 \overline{n} \left(E_i - E_f\right)^3 d_{if}^2}{3\pi\epsilon_0 c^3 \hbar^4}$$

using the optical dipole matrix elements

$$d_{if} = \int \Psi_f(z) \; z \; \Psi_i(z) \; \mathrm{d}z$$

MODEL – The Algorithm Flow-Chart

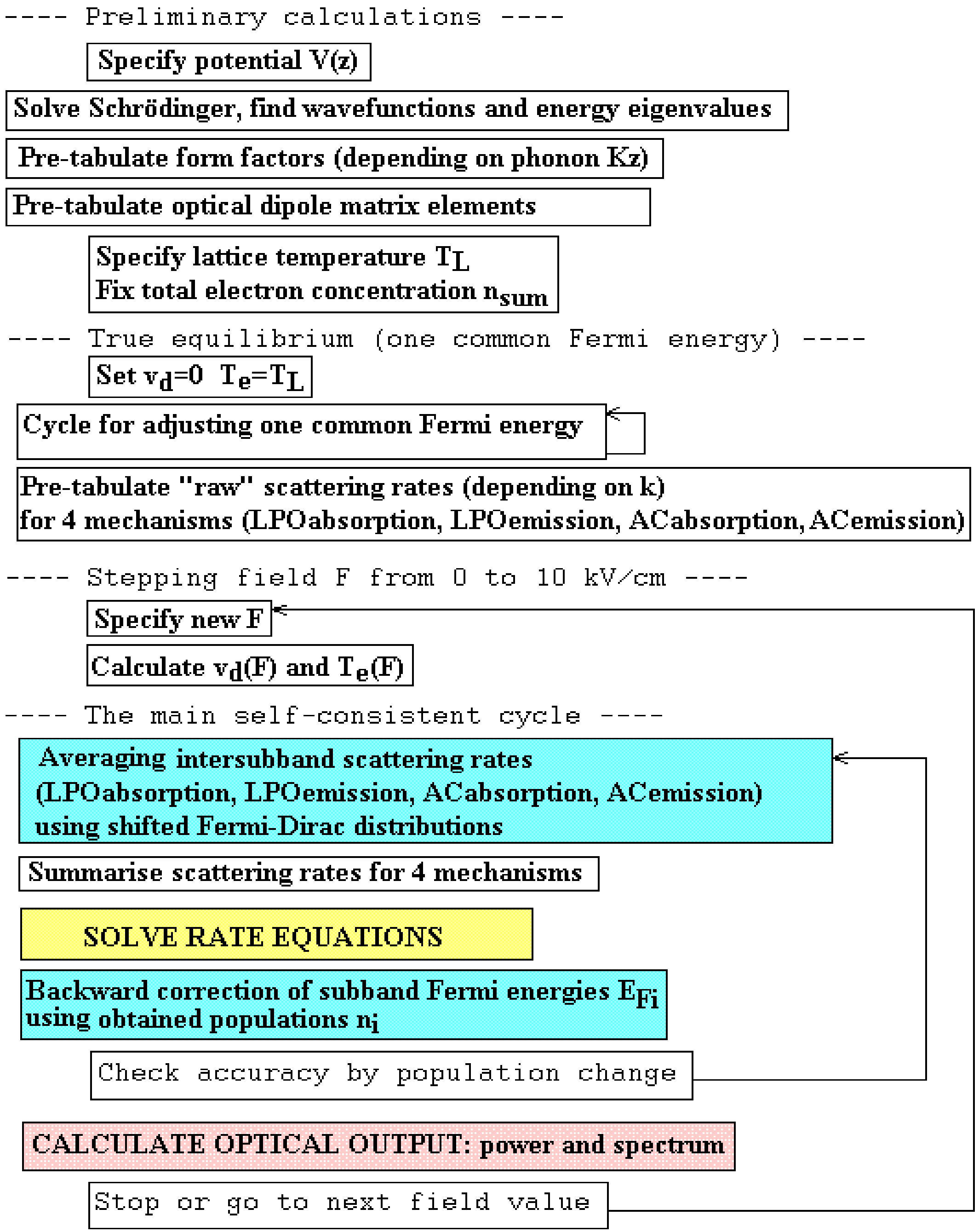

MAIN RESULTS 1 – Subband Populations at different Lateral Fields

FIG. The obtained subband populations versus subband energy at lattice temperature 300K for the quasi-parabolic quantum well with 12 bound states.

The additional 12 continuum states are formed by surrounding the structure with infinite barriers spaced by 200nm. The nearly straight form of curves verifies applicability of Fermi-Dirac (or even Maxwellian) distributions with increased common electron temperature. If the continuum states are omitted then population of bound states increases approximately 10-20% but only at high electron temperatures close to 2000K.

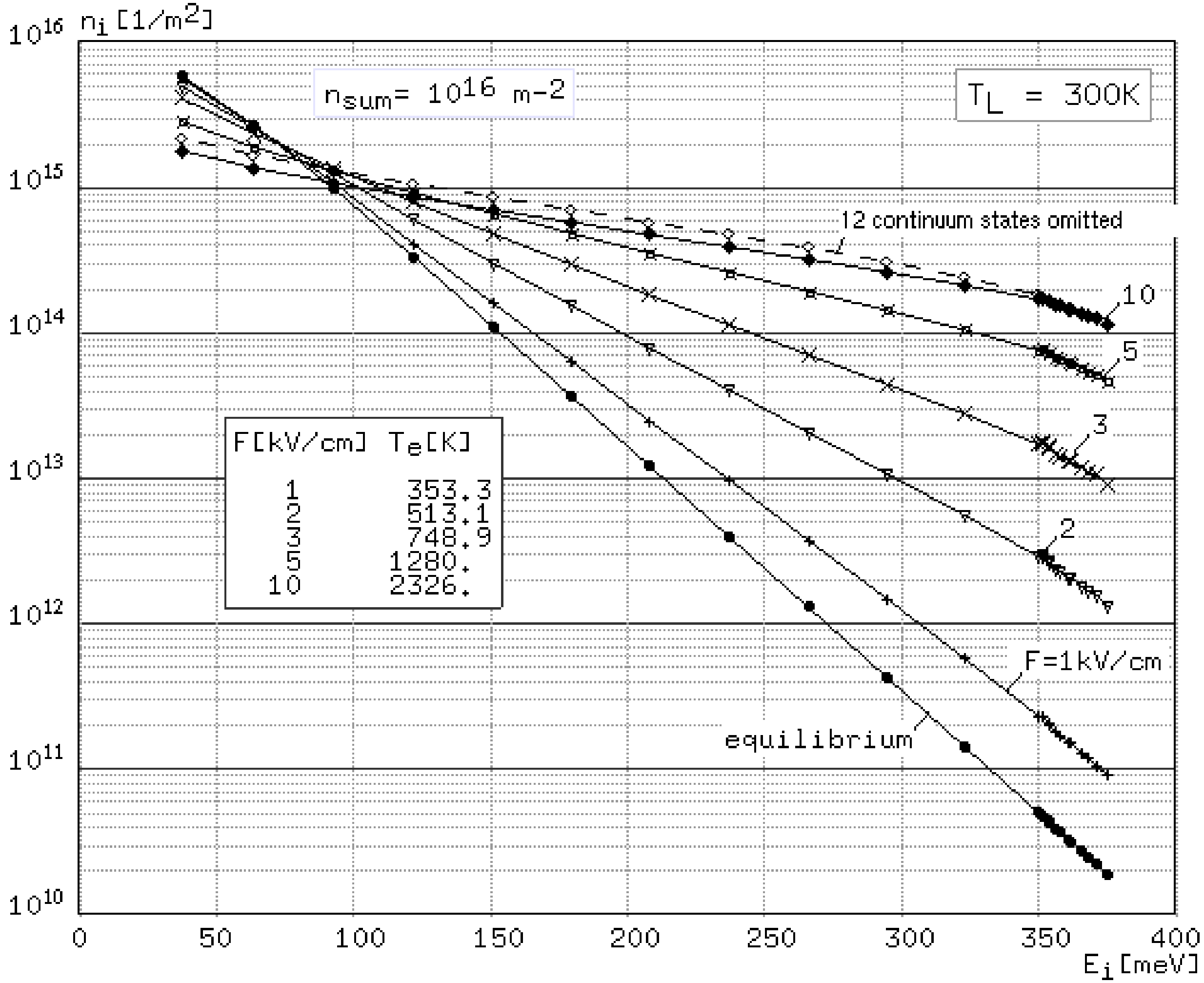

MAIN RESULTS 2 – The Optical Power versus Lateral Field

FIG. The generated radiation power versus lateral electric field for lattice temperatures 77, 300, and 400K.

The smooth parabolic quantum well (with 18% quartic addition) is compared with digitised quasi-parabolic quantum well. The shown blackbody power levels correspond to energy interval 29 ± 5 meV (i.e. ±17% around 7 THz). The inclusion of continuum states decreases the generated power at high fields 15 - 20% due to the decrease of the bound states population densities. The smooth parabolic potential gives approximately 15% higher output power than the digitised potential due to the somewhat greater QW size and respectively greater optical dipole matrix elements.

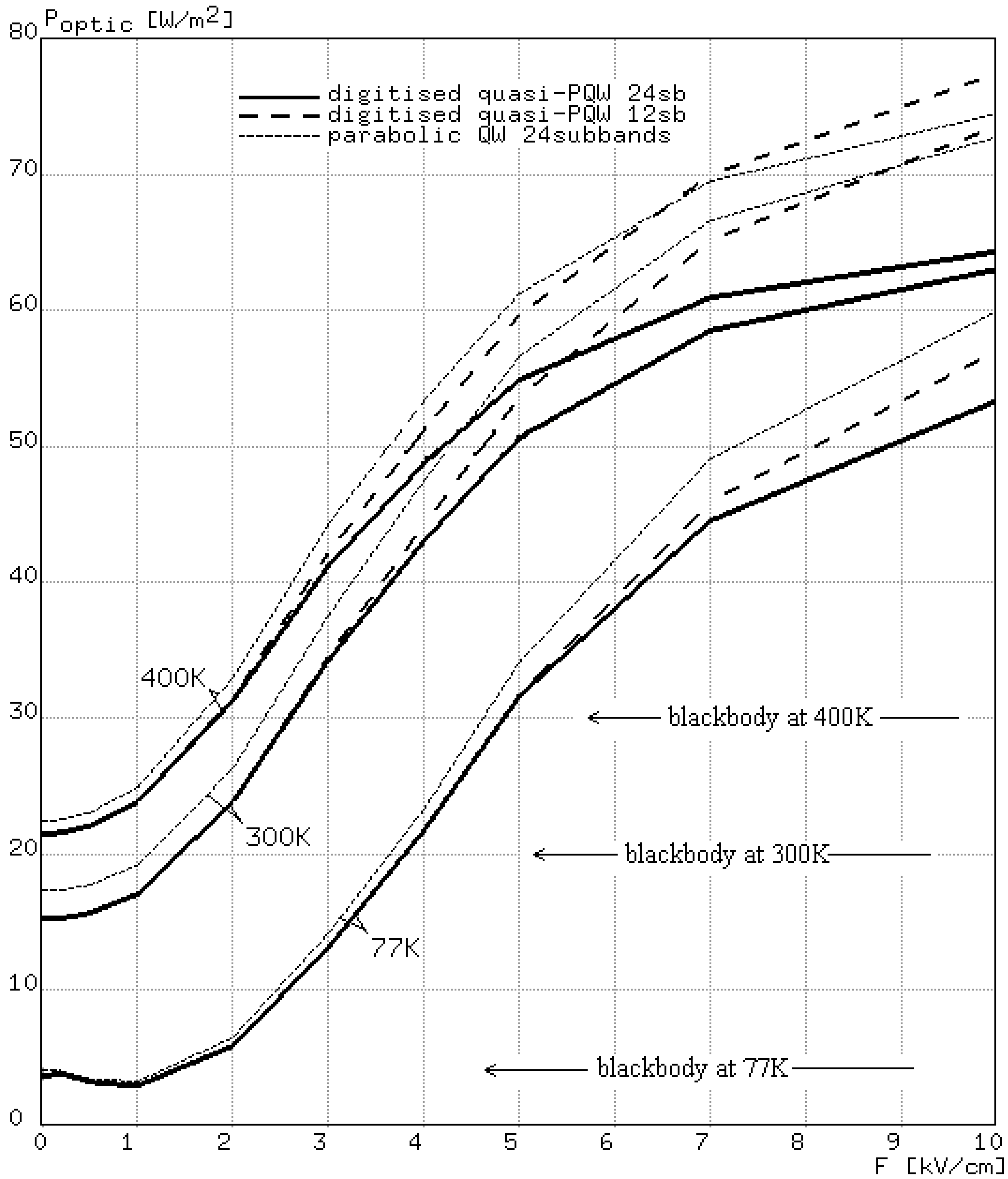

MAIN RESULTS 3 – The Output Spectra Compared with Blackbody

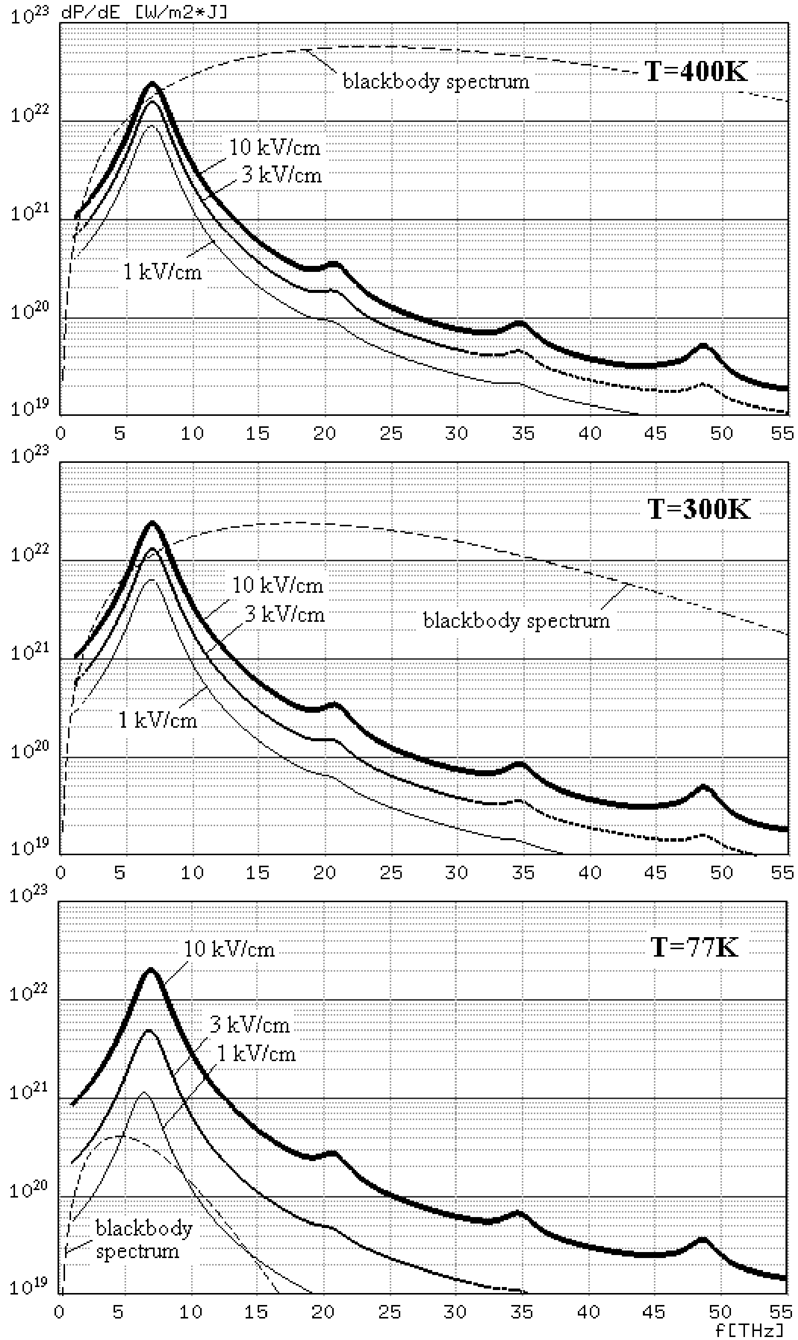

FIG. The generated power spectra for the digitised quasi-parabolic quantum well structure (12 bound states and 12 continuum states) at three lattice temperatures 77, 300, and 400K. The curves for three lateral electric field values are presented and compared with theoretical blackbody spectra.

The Lorentzian linewidth widening (half width at half maximum) parameter Γ is set to 5 meV. The double (even) transitions (14, 28, 42 THz) are excluded due to the wavefunction symmetry properties which yield zero optical dipole matrix elements (ODME). The higher odd transitions (21, 35, 49 THz) have minor importance due to low ODME values compared to adjacent transitions. The closely spaced continuum states give a very low addition since the optical power is proportional to the 4th power of energy spacing between levels.

CONCLUSION

! RESULTS

- Models and methodology developed – a medium-complexity level
- Optical output power estimated is of 60 W/m^2 range – quite low but still over blackbody radiation approximately 2 times at 300K and 1.5 times at 400K
- Basic limitation of optical output – low spontaneous photon emission scattering rate (of 1/μs range) due to the quartic dependence $1/\tau \sim \Delta E^4$ on energy spacing (at 7 THz $\Delta E = 29$ meV)
- A multi quantum layer design may be needed for practical applications

? FURTHER TASKS

- Transfer of the models to a more reliable physical basis – avoid empirical auxiliary parameters, better self-consistent description of the continuum states, check of the accuracy of the shifted Fermi-Dirac distributions etc.
- Study of the possibilities to increase efficiency
- Comparison of the different working frequencies

ACKNOWLEDGEMENTS

Reeno Reeder acknowledges the Estonian Archimedes Foundation for possibility to perform part of his master studies at the Leeds University in autumn 2006.

The authors are grateful to PhD student Nenad Vukmirović from Leeds University for very helpful discussions.

This work and presentation have been supported by the Estonian Science Foundation grants 5911 and 6914. Finally, ITQW07 sponsor organisations support what made possible participation of two authors from Tallinn should not be forgotten.